British Journal of Cancer www.nature.com/bjc

ARTICLE

Cellular and Molecular Biology

HECTD3 regulates the tumourigenesis of glioblastoma by polyubiquitinating PARP1 and activating EGFR signalling pathway

Guanghui Zhang[1], Ruoyue Tan[1], Sicheng Wan[1], Rui Yang[1], Xiaosong Hu[1], Erhu Zhao[1], Xiangfei Ding[2], Jingping Zhang[2], Biao Li[2], Ping Liang[3,4]✉ and Hongjuan Cui[1,2]✉

© The Author(s), under exclusive licence to Springer Nature Limited 2022

BACKGROUND: The E3 ubiquitin ligase HECTD3 is a homologue of the E6-related protein carboxyl terminus, which plays a crucial role in biological processes and tumourigenesis. However, the functional characterisation of HECTD3 in glioblastoma is still elusive.
METHODS: Determination of the functional role of HECTD3 in glioblastoma was made by a combination of HECTD3 molecular pattern analysis from human glioblastoma databases and subcutaneous and in situ injections of tumours in mice models.
RESULTS: This study reports that the DOC domain of HECTD3 interacts with the DNA binding domain of PARP1, and HECTD3 mediated the K63-linked polyubiquitination of PARP1 and stabilised the latter expression. Moreover, the Cysteine (Cys) 823 (ubiquitin-binding site) mutation of HECTD3 significantly reduced PARP1 polyubiquitination and HECTD3 was involved in the recruitment of ubiquitin-related molecules to PARP1 ubiquitin-binding sites (Lysines 209 and 221, respectively). Lastly, activation of EGFR-mediated signalling pathways by HECTD3 regulates PARP1 polyubiquitination.
CONCLUSION: Our results unveil the potential role of HECTD3 in glioblastoma and strongly preconise further investigation and consider HECTD3 as a promising therapeutic marker for glioblastoma treatment.

British Journal of Cancer (2022) 127:1925–1938; https://doi.org/10.1038/s41416-022-01970-9

BACKGROUND

Glioblastoma (GBM) is the most common primary brain tumour [1]. Although radiotherapy, chemotherapy, and surgery have been recognised as treatments for GBM, the prognosis of patients with GBM remains poor with an average of 15 months as life expectancy [2]. In view of this, it is imminently urgent to find out new drug targets for the treatment of GBM to help improve the life and extend the longevity of patients affected by GBM [3].

Ubiquitination is a posttranslational modification of proteins playing an essential role in several biological processes, such as protein fate determination, signal transduction, cell growth, and sequential reactions. The latter is catalysed by key ubiquitin-related enzymes, including ubiquitin-activating enzyme (E1), ubiquitin-conjugating enzyme (E2), and ubiquitin ligase (E3), whom the catalytic action led to a covalent conjugation between ubiquitin-related molecules and targeted proteins [4–6]. It has been reported that the target proteins are generally connected by a ubiquitin chain formed by both glycine and Lys residues at the C-terminus, on one hand, and ubiquitin-related molecules connected to several Lys' sites (sites 6, 11, 27, 29, 33, 48, and 63, respectively), on another hand [7, 8]. The E3 ubiquitin ligase HECTD3 is homologous with the carboxyl end of the E6-related protein belonging to the HECT-type ubiquitin ligase [4], which contains both the DOC binding domain and HECT ubiquitin domain [9]. HECTD3 plays an important role in several biological processes and tumourigenesis. Previous studies have shown that HECTD3 catalyses the ubiquitination-based degradation of the actin-related repeat Tara and may target syntaxin-8 to cause neurodegenerative diseases [10, 11]. Recent studies have indicated that HECTD3 mediates the formation of non-K48-linked polyubiquitin chains on STAT3, caspase-8 and caspase-9, MALT1, and TRAF3 [9, 12–16] as well as the occurrence and progression of cerebrospinal diseases and cancer. With the in-depth studies of HECTD3, increasing evidence shows that HECTD3 is highly expressed in ovarian cancer, breast cancer, and oesophageal squamous cell carcinoma and promotes the proliferation of tumour cells [12, 13, 17]. Altogether, these findings show that HECTD3 plays a crucial role in tumour progression. However, the biological function of HECTD3 in GBM remains unclear.

Studies have shown that the nucleolus plays an important biological role in ribosome biogenesis, and increasing evidence has indicated that the nucleolus, as a regulatory centre, is involved

[1]State Key Laboratory of Silkworm Genome Biology, Southwest University, 400716 Chongqing, China. [2]Cancer Center, Medical Research Institute, Southwest University, 400716 Chongqing, China. [3]Department of Neurosurgery, Children's Hospital of Chongqing Medical University, National Clinical Research Center for Child Health and Disorders, Ministry of Education Key Laboratory of Child Development and Disorders, 400014 Chongqing, China. [4]Chongqing Key Laboratory of Pediatrics, 400014 Chongqing, China.
✉email: pingliangnet@163.com; hongjuan.cui@gmail.com

Received: 26 January 2022 Revised: 18 August 2022 Accepted: 23 August 2022
Published online: 10 September 2022

in the occurrence and development of many cancers, including DNA damage repair, cell apoptosis, cell cycle control, and protein stability [18]. Interestingly, poly (ADP ribose) polymerase 1 (PARP1) is located in the nucleolus and is reported to play a crucial role in cancer biology via several processes, including genome stabilisation, replication, transcription, and chromatin remodelling [18]. Furthermore, it has been reported that the combination of inhibitors targeting PARP1 and radiotherapy slows tumour recurrence in GBM mice [19]. Since existing targets for GBM control are limited, it is urgent to find out new therapeutic targets, including those of PARP1. The transmembrane receptor epidermal growth factor receptor (EGFR) is a transmembrane receptor and a glycoprotein with a tyrosine kinase activity [20]. Studies have shown that EGFR is highly expressed in GBM, and this expression occurred in 30–40% of GBM patients [2, 21–23]. Besides, abnormal expression of EGFR was associated with GBM proliferation, invasion, and recurrence [24, 25]. Previous studies have shown that the inactivation of PARP1 inhibited the activation of the EGFR signalling pathway [26].

In this study, our results revealed that HECTD3 is involved in GBM cell proliferation, apoptosis, DNA damage, and migration. Mechanistically, we showed that HECTD3 and PARP1 interact with each other through their respective DOC and DNA-binding domains. We further reported that HECTD3 mediates the K63-linked polyubiquitination of PARP1 and stabilises PARP1 expression by recruiting ubiquitin-related molecules to PARP1 key amino acid sites (Lys209 and Lys221). Moreover, HECTD3 activates the EGFR-based signalling pathway by regulating PARP1 polyubiquitination. Taken together, this study shows that HECTD3 may be considered a therapeutic target in patients with GBM, and hence provides a theoretical basis for clinical research on GBM.

METHODS

Cell lines and cell culture

All human GBM cell lines (LN229, U87MG, U118, and A172), human astroglial cells SVGP12, and human embryonic kidney (HEK) 293 cells were obtained from American Type Culture Collection [3]. The above cells were cultured in a DMEM medium with 10% foetal bovine serum (FBS). All cell lines were authenticated by short-tandem repeat analysis. Primary glioblastoma GBM-3 cells were obtained from Daping Hospital (Chongqing, China) and were cultured in DMEM/F-12 medium with 10% FBS [27]. These cell lines were mycoplasma-free (checked by using a Mycoplasma Stain Assay Kit named C0296, Beyotime Biotechnology, Shanghai, China), and cultured in a humidified environment supplemented with 5% CO_2 at 37 °C.

Reagents, antibodies, and clinical tissue samples

MG132 and CHX were obtained from Sigma (Shanghai, China). A rabbit-enhanced polymer detection system (#PV-9001) for immunohistochemistry (IHC) was purchased from ZSGB-Bio (Beijing, China). Alexa Fluor 594-labelled secondary antibody (#A11034) and Hoechst 33342 (#H1399) were purchased from Thermo Fisher (Shanghai, China). The antibodies used include the following: 11487-1-AP (anti-HECTD3), 10122-1-AP (anti-CDK2), 11026-1-AP (anti-CDK4), 66031-1-Ig (anti-α-Tubulin), 60003-2-Ig (anti-MYC-Tag), 66006-2-Ig (anti-HA-Tag), 66008-4-Ig (anti-Flag-Tag), and 27309-1-AP (anti-Ki67) were purchased from Proteintech (Wuhan, China). The HECTD3 antibody (bs-15448R) was obtained from Bo Aosen Biotechnology Co., Ltd (Beijing, China). Antibodies against PARP1 (#9532), Cleaved-PARP1 (#5625), Caspase3 (#9662), Cleaved-caspase3 (#9661), EGFR (#2085), phospho-EGFR (#3777), and phospho-AKT (#4060) were purchased from Cell Signalling Technology (Shanghai, China). Antibodies against PARP1 (ab227244 and ab157046) were purchased from Abcam (Shanghai, China). Antibody dilutions' information is available in Supplementary Table 3. Clinical glioma tissue samples were purchased from Chaoying Biotechnology Co., Ltd. (Xian, China).

IHC and haematoxylin and eosin (H&E) staining

Paraffin-embedded tumour tissues were sectioned at 6 μm, and then the paraffin sections and clinical glioma samples were dewaxed and hydrated. Then, paraffin slices were put into citrate buffer (pH 6.0) and heated (95 °C/20 min) to facilitate antigen retrieval. Afterward, endogenous peroxidase activity was blocked, and goat serum was applied to tumour tissue sections and clinical glioma samples to block nonspecific binding, before overnight (4 °C) incubation with PBS-diluted HECTD3, EGFR, PARP1, and Ki67 primary antibodies. Then, a horseradish peroxidase-linked secondary antibody was added to the above samples for further incubation and stained with DAB. After haematoxylin re-staining, hydrochloric acid acidification, ammonia anti-blue, dehydration, and sealing, photos were taken for observation. For H&E staining, paraffin-embedded mice tumour tissue in situ was sectioned at 10 μm, and then the paraffin sections were dewaxed and hydrated. Samples were then stained with haematoxylin, followed by counterstaining with eosin, before microscopic visualisation of results.

Plasmids, lentivirus packaging, and infection experiments

Small hairpin shRNAs for HECTD3 and PARP1 and a negative control shRNA (shGFP) were obtained from Gene Pharma Co. Ltd. (Shanghai, China) and were inserted into the pLKO.1 vector. The ubiquitination plasmids contained HA-Ubs (K6R, K11R, K27R, K29R, K33R, K48R, and K63R) and HA-Ub-WT were cloned into the pCDH-CMV-MCS-EF1-GFP-Puro vectors and pRK5 vectors respectively, which were purchased from Youbao Company (Changsha, China). The recombinant plasmids containing human Flag-HECTD3, MYC-PARP1 and Flag-HECTD3 (amino acids 1–511), Flag-HECTD3-1-511 (amino acids ΔH215–393), MYC-PARP1 (amino acids 1–380) and MYC-PARP1 (amino acids 511–1014) were cloned into the pCDH-CMV-MCS-EF1-GFP-Puro vector and purchased from Youbao Company (Changsha, China). The GST-Flag-HECTD3 plasmid was cloned into the PGEX-6p-1 vector and purchased from Youbao Company (Changsha, China). Flag-HECTD3 (amino acids 512–861), Flag-HECTD3 (amino acids 215–393), and MYC-PARP1 (amino acids 381–510) were cloned into the pCDH-CMV-MCS-EF1-GFP-Puro vector. MYC-PARP1-K209R, MYC-PARP1-K221R, MYC-PARP1-K548R, MYC-PARP1-K579R, and MYC-PARP1-K667R plasmids were cloned into the pCDH-CMV-MCS-EF1-GFP-Puro vector and purchased from Jinkairui Bioengineering Co., Ltd (Wuhan, China). For lentivirus packaging and infection assays, the target plasmid (500 ng) and packaging plasmid (PLP1, PLP2, and VSVG)/500 ng were co-transfected into 293 cells in one six-well plate by using the transfection reagent Lipofectamine 2000 (Invitrogen, Carlsbad, CA, USA). Lentiviruses were collected 48 h later and used to infect GBM cells twice, 12 h per infection. The infected cells were screened by treatment for 48 h with puromycin, and the surviving cells were frozen and stored in liquid nitrogen for subsequent assays.

Animal models and tumour xenograft

Four-week-old female nude mice were purchased from Huafukang Biotechnology Co., Ltd. (Beijing, China). Mice were randomly assigned to receive subcutaneous injections, and divided into five groups (6 mice/group) and two groups (4 mice/group). Briefly, stably transfected GBM cells (U87MG) (1×10^6 cells) with shGFP, shHECTD3#1, shHECTD3#2, shHECTD3/GFP, shHECTD3/HECTD3, shGFP, and shPARP1 were collected and resuspended in 100 μl PBS before to be injected into the subcutaneous tissue of the mice. Before subcutaneous injection, mice were anaesthetised with an isoflurane nasal anaesthesia system to reduce pain. Before collecting the tumour, mice were anaesthetised with isoflurane nasal anaesthesia system and euthanised through cervical dislocation. Then, mice corpses were collected and stored at −20 °C and sent to Laibite Biotechnology Co., Ltd. (Chongqing, China) for incineration. Tumour volumes were calculated by using the following formula: $V = (\text{length} \times \text{width}2)/2$. As described previously [23, 28], mice were divided into two groups, one group (3 mice/group) was used for H&E staining and IHC assay, the other group (5 mice/group) was monitored for survival. Mice were anaesthetised using an isoflurane nasal anaesthesia system to reduce the pain caused by in situ injections, and GBM cells (U87MG) (1×10^5 cells) were stably transfected with shGFP, shHECTD3, and shHECTD3/PARP1, collected and resuspended in 6 μl PBS and then injected into the brains of mice. Before collecting the brains of mice, mice were further anaesthetised and euthanised through cervical dislocation. Similarly, mice corpses were collected and stored at −20 °C and sent to Laibite Biotechnology Co., Ltd. (Chongqing, China) for incineration. Animal handling was approved by the Committee for Animal Protection and ethics of Southwest University. All experiments were conducted following the Guidelines for Animal Health and Use of the Ministry of Science and Technology of China (2006).

Western blot assay
Cells were lysed with RIPA lysis buffer, and the released proteins were separated on 10, 12, and 15% polyacrylamide electrophoresis gels, respectively. Gels were transferred to a polyvinylidene difluoride membrane, which was blocked with 5% BSA and nonfat milk powder at room temperature for 2 h. Thereafter, the polyvinylidene fluoride membrane was overnight incubated (4 °C) with a diluted primary antibody, followed by a second incubation with a secondary antibody (peroxidase-labelled anti-mouse and anti-rabbit antibodies) at room temperature for 2 h. Finally, the results were analysed with the ECL Prime western blot (WB) detection system (GE Healthcare).

Immunoprecipitation (IP) assay
The IP assay was performed as described previously [3]. Briefly, cells were collected and lysed with IP lysis buffer. Then, protein A/G magnetic beads were preincubated with the different antibodies. Cell lysates were overnight incubated (4 °C) with antibody-coupled beads. The beads were washed and then denatured at 100 °C, and the proteins were detected by western blot.

Ubiquitination and turnover assay
Constructed plasmids, shGFP, Flag-HECTD3, Flag-HECTD3 (C823A), PARP1, and HA-Ubs (WT, K6R, K11R, K27R, K29R, K33R, K48R, and K63R) plasmids were transfected into 293 cells by using the transfection reagent Lipofectamine 2000 (Invitrogen, Carlsbad, CA, USA). Forty-eight hours post-transfection, 50 μg/ml of the proteasome inhibitor MG132 was added to the cells and incubated for 7 h. The cells were collected and lysed with IP lysis buffer. The cell lysates were overnight incubated at 4 °C with antibody-coupled beads. The beads were washed, denatured at 100 °C, and the proteins were detected by western blot. For the turnover assay, the infected cells were screened for 48 h with puromycin, and the surviving cells were treated with CHX at a concentration of 50 μg/ml. Finally, the cells were collected, lysed, and analysed by western blot.

BrdU staining
For this assay, 2×10^4 cells were cultured in 24-well plates, followed by 30 min with 10 μg/ml BrdU. Then the samples were fixed with paraformaldehyde, acidified with hydrochloric acid, and blocked with goat serum. Samples were successively incubated with a primary antibody (anti-BrdU; Abcam, Cambridge, MA, USA) overnight (4 °C), and a secondary antibody (Alexa Fluor® 594; H + L; Invitrogen™) at room temperature for 2 h, respectively. Thereafter, nuclear staining was performed with DAPI (300Nm), and the BrdU incorporation rate was calculated from at least three randomly chosen microscopic fields.

Cell proliferation detection and plate colony formation experiment
To test the cell proliferation ability, 1×10^3 cells were cultured in both 96- and 6-well plates for 6 and 15 days, respectively. As described previously [28], cell viability was detected by using the MTT assay. The plate clone formation assay was scanned after crystal violet staining, finally, the absorptivity at 560 nm was measured by absolute ethanol for statistical analysis. All experiments were performed three times, independently.

Quantitative reverse transcriptional PCR (qRT-PCR)
As described previously [28], total RNA was extracted through TRIzol reagent (Invitrogen™), and 2 μg of RNA were reverse transcribed into cDNA. SYBR qPCR SuperMix Plus was used for qRT-PCR (Novoprotein, China). The primer pairs were shown in Supplementary Table 1. Results were calculated using the ΔΔCt method with glyceraldehyde-3-phosphate dehydrogenase serving as the internal control [29].

Flow cytometry analysis
For apoptosis analysis, puromycin was used to select lentivirus-infected cells. After 2 days of screening, as described previously [30], cells were collected for incubation with FITC-labelled annexin V and propidium iodide (PI) at room temperature for 25 min before being analysed by the FACS C6 flow cytometry (BD, USA).

Proximity ligation assay (PLA) and immunofluorescence (IF) assay
The cells infected with lentivirus were successively screened with puromycin, fixed with paraformaldehyde, blocked with goat serum, and finally overnight incubated overnight with γ-H2AX, Flag, and PARP1 antibodies. Next, the cells were incubated with an Alexa Fluor 594-labelled secondary antibody (1:1000) and a PLA assay Kit (Sigma-Aldrich®). Finally, the cells were visualised and photographed with a confocal fluorescence microscope. Thanks to Jifu Li for providing technical support during the use of the Confocal Laser Scanning Microscope (Olympus Fv1000, Japan).

Migration and wound healing assays
Cell migration experiments were carried out in the Transwell chambers. The cells' mean number was calculated from at least three randomly chosen microscopic images. For the wound healing assay, the cells were cultured in 6-well plates, and then the wound was made with a 10-μl pipette tip, and wound healing was microscopically observed, randomly.

Patient database analysis
All data sets were obtained from CGGA (http://www.cgga.org.cn/), GEPIA (http://gepia.cancer-pku.cn/index.html), and GlioVis (http://gliovis.bioinfo.cnio.es/) databases, respectively.

Statistical analysis
Triplicates at least were designed and performed in each of the above experiments. Statistical parameters (sample size and significance analysis) are shown in the legend. Data were analysed and shown as mean ± SD. Statistics analyses were performed using GraphPad Prism 8.0. Two-tailed Student's *t* tests were performed for paired samples. $^*p < 0.05$, $^{**}p < 0.01$, and $^{***}p < 0.001$ were considered to indicate statistical significance.

RESULTS
HECTD3 is highly expressed in GBM tissues and associated with a poor prognosis
To explore the role of HECTD3 in GBM, we first performed an IHC assay to detect the expression of HECTD3 in 5 normal brain tissue samples and 35 glioma patient samples. The results showed that HECTD3 expression gradually increased in a grade-dependent manner in normal and glioma tissues (Fig. 1a, b). Then, we performed a succession of bioinformatics analyses to detect, compare and confirm the above finding. Analysis of CCGA databases showed that HECTD3 expression was increased in a grade-dependent manner and HECTD3 was highly expressed in GBM (Fig. 1e). Moreover, analysis of the histology and age-based expression of HECTD3 were analysed through the CGGA database revealed that HECTD3 was significantly expressed in both recurrent and non-recurrent GBMs (Fig. 1c), with a particularly high expression in patients with grade IV GBM, aged at least 42 years old (Fig. 1d). Further analysis results that indicate the tissues where HECTD3 expression was higher, as well as the GBM grade levels and the IDH mutational status, are embedded in the supplementary materials (Fig. S1A–D). Interestingly, analysis of the possible association between patient prognosis and HECTD3 expression in different grades of gliomas through the CGGA database showed an association between HECTD3 high expression and different glioma grades with poor prognosis (Fig. 1f–i). To get more insights into the role of HECTD3 in GBM, we detected HECTD3 protein expression levels in human astrocytes (SVGP12), primary glioblastoma (GBM-3), and GBM (U87MG, LN229, U118, A172) cell lines through western blot assay. The results indicated that HECTD3 was highly expressed in GBM cells (Fig. 1j), and LN229, U87MG, and GBM-3 cell lines were used in subsequent experiments. To sum up, these data suggest that HECTD3 is highly expressed in GBM and might play an oncogenic function.

Knockdown of HECTD3 inhibited the proliferation and migration ability of GBM cells
To further elucidate the effect of HECTD3 on GBM cell proliferation. Two independent short hairpin RNAs (shRNA#1 and shRNA#2) were designed to knock down HECTD3 expression in LN229, U87MG, and GBM-3 cell lines. Western blot and qRT-PCR analyses showed that HECTD3 expression was successfully

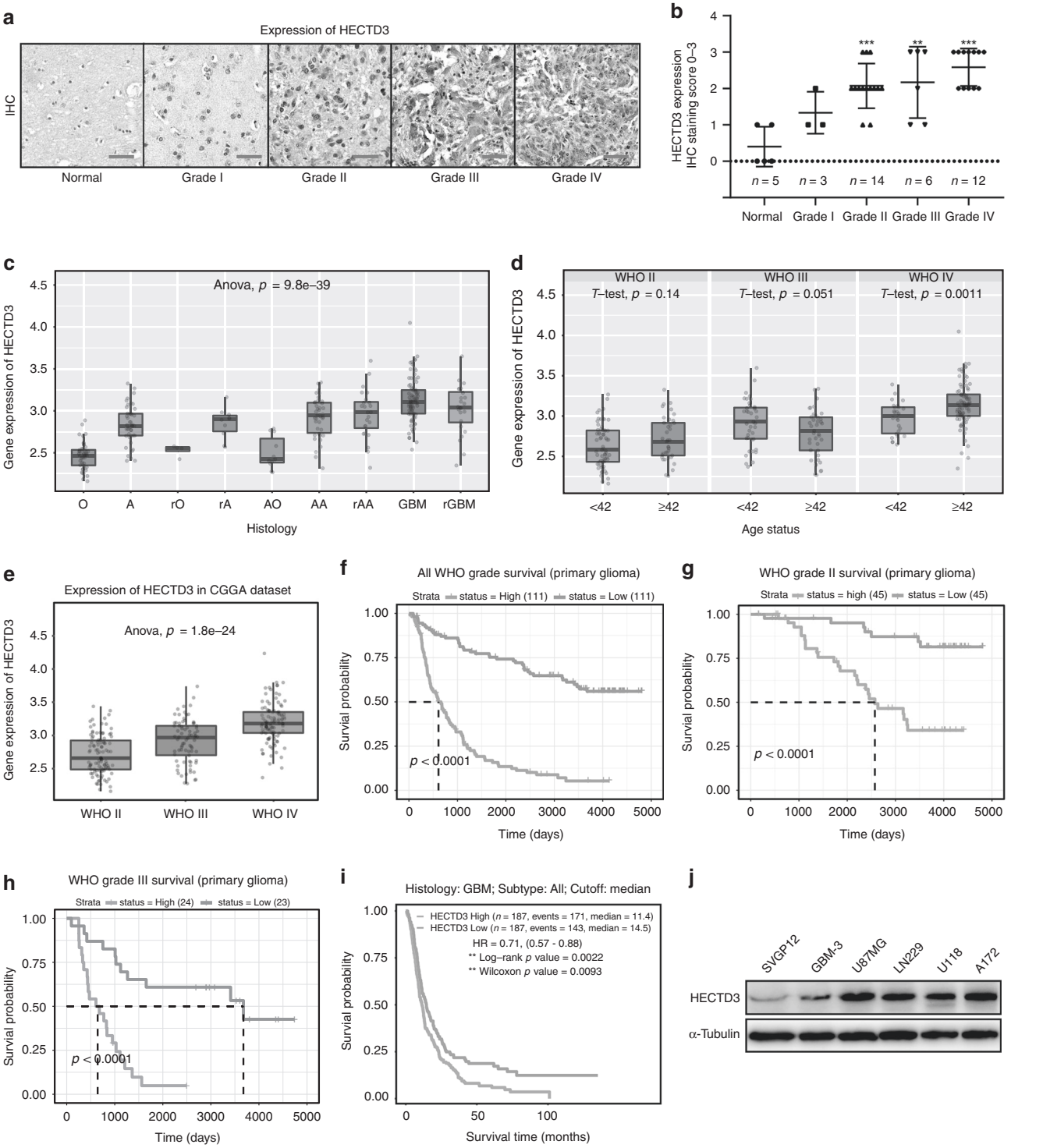

Fig. 1 HECTD3 is highly expressed in GBM tissues and associated with a poor prognosis. a Immunohistochemical staining analysis was used to detect the expression of HECTD3 in normal brain tissues and glioma tissue samples. **b** Statistical analyses of HECTD3 in 5 normal brain tissue samples and 35 glioma patient samples. **c**–**e** The CGGA (http://www.cgga.org.cn/) database was used to analyse the expression of HECTD3 in different grade gliomas, histology and age status. **f**–**i** The CGGA (http://www.cgga.org.cn/) and GlioVis (http://gliovis.bioinfo.cnio.es/) databases were used to analyse the prognosis of HECTD3 in patients with different grades of glioma. **j** The protein expression of HECTD3 in human astrocytes cell (SVGP12), primary glioblastoma cells GBM-3 and GBM cell lines (U87MG, LN229, U118, A172) cell lines. All data were expressed as mean ± SD. Student's *t* test was performed to analyse significance. $^{**}p < 0.01$, $^{***}p < 0.001$.

knocked down (Fig. 2a). Then, we examined the proliferation abilities of LN229, U87MG and GBM-3 cells by MTT assay, and revealed that knocking down HECTD3 expression significantly inhibited the proliferation of above-cited cell lines (Fig. 2b). We next sought to determine the DNA synthesis amount by using the BrdU incorporation assay. We found that the DNA synthesis level was significantly reduced in HECTD3-knocked-down LN229, U87MG, and GBM-3 cells in comparison to control cells

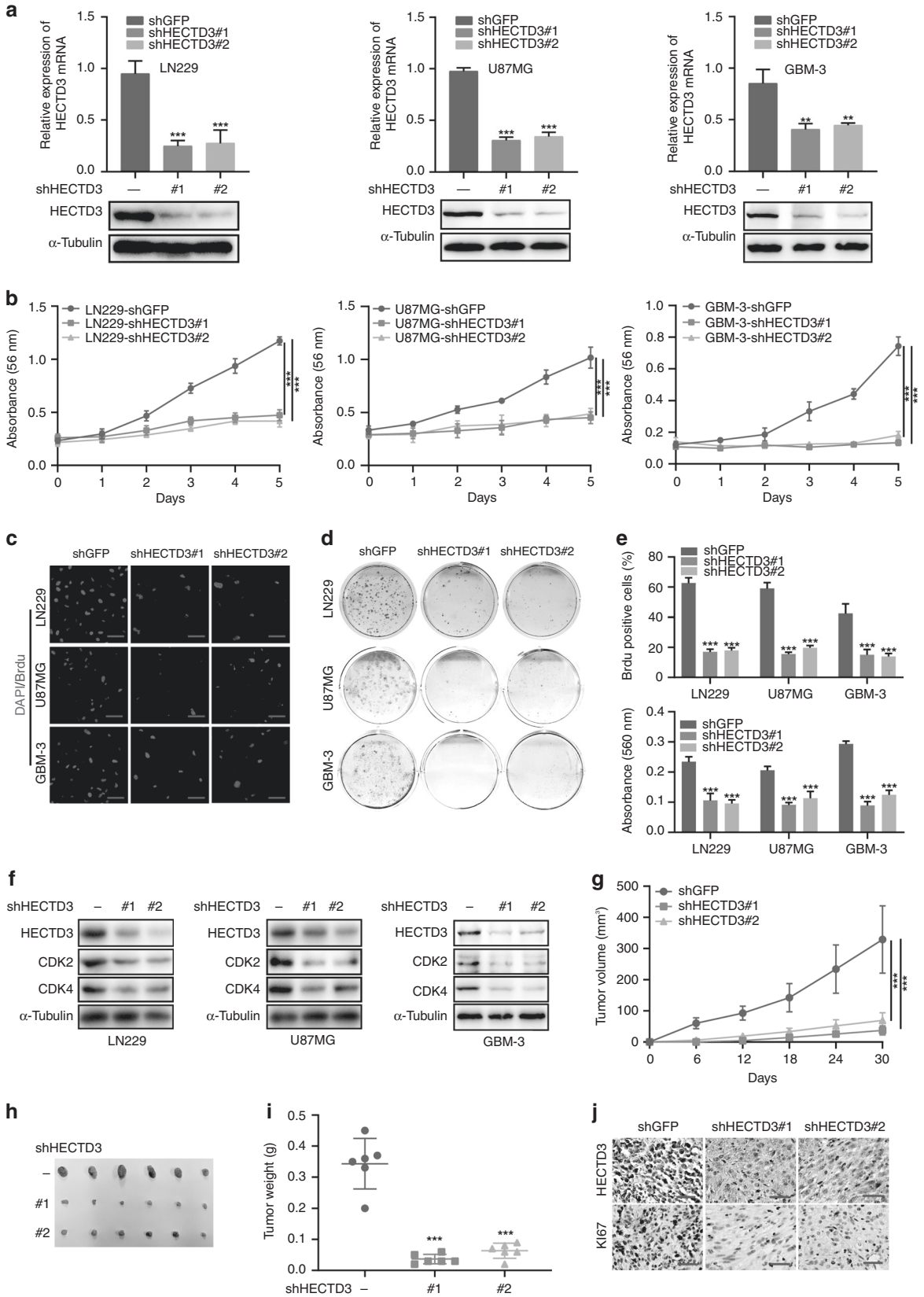
a
Relative expression of HECTD3 mRNA
shGFP
shHECTD3#1
shHECTD3#2
LN229
U87MG
GBM-3
shHECTD3
HECTD3
α-Tubulin
b
LN229-shGFP
LN229-shHECTD3#1
LN229-shHECTD3#2
U87MG-shGFP
U87MG-shHECTD3#1
U87MG-shHECTD3#2
GBM-3-shGFP
GBM-3-shHECTD3#1
GBM-3-shHECTD3#2
Absorbance (56 nm)
Days
c
DAPI/Brdu
d
e
Brdu positive cells (%)
Absorbance (560 nm)
f
CDK2
CDK4
g
Tumor volume (mm³)
h
i
Tumor weight (g)
j
KI67

Fig. 2 Knockdown of HECTD3 inhibited the proliferation and migration ability of GBM cells. a qRT-PCR assay and western blot assays were used to detect HECTD3 expression in HECTD3-knocked-down LN229 and U87MG cells. **b** Growth curves of knocked down HECTD3 LN229 and U87MG cells. **c**, **e** Image and quantification of LN229 and U87MG cells positive for BrdU staining are shown after knocking down HECTD3. **d**, **e** The plate colony formation ability of LN229 and U87MG cells with HECTD3 knockdown. **f** Protein expression levels of HECTD3, CDK2, CDK4, and α-Tubulin were detected by western blot in HECTD3-knocked-down LN229 and U87MG cells. **g** The growth curve of tumours was examined for HECTD3-knocked-down U87MG cells that were subcutaneously injected into nude mice**. h**, **i** The size and weight of xenograft tumours were analysed in mice injected with HECTD3-knocked-down U87MG cells. **j** Expression levels of HECTD3 and Ki67 in HECTD3-knocked-down tumours were detected by immunohistochemistry. All data were expressed as mean ± SD. Student's *t* test was performed to analyse the significance. $^{**}p < 0.01$, $^{***}p < 0.001$.

(Fig. 2c, e). This corroborates with the reduced cell colony numbers observed with HECTD3-knocked-down cells in consideration to those of the control groups when performing the plate cloning assay (Fig. 2d, e). Next, to detect the effect of HECTD3 on the cell cycle, we applied a western blot assay to check the cell cycle-related protein expression levels. As shown in Fig. 2f, expression levels of cell cycle proteins CDK2 and CDK4 were reduced in HECTD3 knocked down cells in comparison to control ones. Then, xenograft experiments indicated that the tumour growth rate, volume, and weight in HECTD3-knocked-down U87MG cells were significantly decreased compared to those in the control groups (Fig. 2g–i). Besides, HECTD3 and Ki67 expression levels were significantly decreased in HECTD3-knocked-down tumour cells compared to controls, as revealed by IHC (Fig. 2j). Subsequently, transwell assays and wound healing assays were performed to detect the migration ability of GBM cells in HECTD3-knocked-down LN229 and U87MG cells. The results indicated that the migration ability was decreased in HECTD3-knocked-down GBM cells compared to the control groups (Fig. S2A, B). We further explored the migration-related protein expression levels using a western blot assay. Figure S2C shows reduced expression levels of Slug and MMP2 proteins in HECTD3-knocked-down LN229 and U87MG cells. Taken together, these results suggest that HECTD3 played an important role in GBM and is involved in the proliferation and migration of GBM cells.

HECTD3 is required for GBM cells proliferation

The above findings showed that knockdown of HECTD3 inhibited the proliferation and migration ability of GBM cells. To investigate whether this inhibition was occasioned by an off-target effect, we restored the expression of HECTD3 in the knocked-down cells (LN229, U87MG, and GBM-3), and found via western blot the functional rescue of HECTD3 as well that of the cell cycle-related proteins CDK2 and CDK4, respectively (Fig. 3a). Furthermore, through MTT, BrdU incorporation, and plate colony formation assays, our results showed that the restoration of HECTD3 expression after its knockdown rescued the inhibition of GBM cell proliferation previously shown to be caused by HECTD3 knockdown to a great extent (Fig. 3b–e). Then, we carried out the subcutaneous tumourigenesis in a mice model and reported that restored HECTD3 expression was considerably associated with rescuing the subcutaneous tumourigenicity of U87MG cells (Fig. 3f, g). Similar results were obtained after performing the IHC assay, which indicated a significantly restoration of HECTD3 and Ki67 expression levels (Fig. 3h). To get more insights into the HECTD3 effect on GBM cell proliferation, we over-expressed HECTD3 in GBM cells followed by a western blot assay, which indicated that the cell cycle-related proteins (CDK2 and CDK4) expression levels were increased in GBM cells overexpressing HECTD3 compared to the control cells (Fig. 3i). A proliferation of LN229 and U87MG cells were observed in GBM cells over-expressing HECTD3 when repeating the MTT and plate colony formation assays (Fig. 3j, k). Taken together, these results showed that HECTD3 promotes the proliferation of GBM cells and might serve as a promising target for GBM treatment.

The DOC domain of HECTD3 interacts with the DNA-binding domain of PARP1

To further explore the mechanism by which HECTD3 promotes the proliferation of GBM cells, we applied a mass spectrometric analysis targeting HECTD3 and found that the latter interacted with PARP1. When we performed an IP assay, the results confirmed the interaction of HECTD3 with PARP1 in LN229, U87MG, and GBM-3 cells (Fig. 4a) to further prove the direct interaction between HECTD3 and PARP1. This finding was further supported by using proximity Ligation (PLA) and GST-pull down assays in GBM cells (Figs. 4b and S3A). We next sought to characterise which domain(s) mediated the interaction between HECTD3 and PARP1. HECTD3 was truncated as the following: amino acids from 1–511 (DOC domain), 215–393, ΔH215–393, and 512–861 (HECT domain) (Fig. 4c). Truncated Flag-tagged DOC and HECT domains as well as the full-length MYC-tagged PARP1 were transiently co-transfected with HEK293 cells, and we found that the HECTD3 DOC domain interacted with PARP1 (Fig. 4d). As well, we investigated the PARP1 domain interacting with the HECTD3 DOC domain. PARP1 was first truncated into several peptides 1–380 aa (DBD), 381–510 aa (AD), and 511–1014 aa (CAT) (Fig. 4e), then MYC-tagged PARP1 truncated domains and Flag-tagged HECTD3 DOC domain with immunoprecipitates from transiently transfected HEK293 cell lysates. The results indicated that the HECTD3 DOC domain interacted with the PARP1 DBD domain (Fig. 4f).

Depletion of HECTD3 reduces the expression of PARP1 and induces apoptosis and DNA damage in GBM cells

Studies have shown that PARP1 is abnormally expressed in GBM cells and promotes the proliferation of the latter. Investigation of Gene Expression Profiling Interactive Analysis (GEPIA) and CGGA gene database analysis showed that PARP1 is highly expressed in GBM patients with a poor prognosis (Fig. S4A, B). Then, an IHC assay was performed to detect the expression of PARP1 in 5 normal brain tissue samples and 35 glioma patient samples. The results showed that PARP1 expression gradually increased in a grade-dependent manner (Fig. 5a). Two independent shRNAs (shRNA#1 and #2) were designed to knock down PARP1 expression in LN229 and U87MG cells. We revealed by western blot assay that the expression of PARP1 was successfully knocked down (Fig. S4C). Then, xenograft experiments suggested that the volume and weight of tumours and the growth rate of tumours in PARP1 knockdown U87MG cells were significantly decreased compared with those in the control groups (Fig. 5b, c). We previously demonstrated that HECTD3 interacts with PARP1. To further explore the regulatory effect of HECTD3 on PARP1, we assessed, via western blot and qRT-PCR assays, the relative expression level of PARP1. We found that PARP1 protein expression was reduced, whereas that of the cleaved PARP1 protein increased in HECTD3 knocked-down LN229, U87MG, and GBM-3 cells (Figs. 5d and S4E). However, the mRNA expression of PARP1 was not significantly changed in HECTD3 knocked-down GBM cells (Fig. S4D). Hence, we assumed that HECTD3 could regulate the expression of PARP1 via ubiquitination. PARP1 plays an important role in DNA damage repair, cell apoptosis, cell cycle

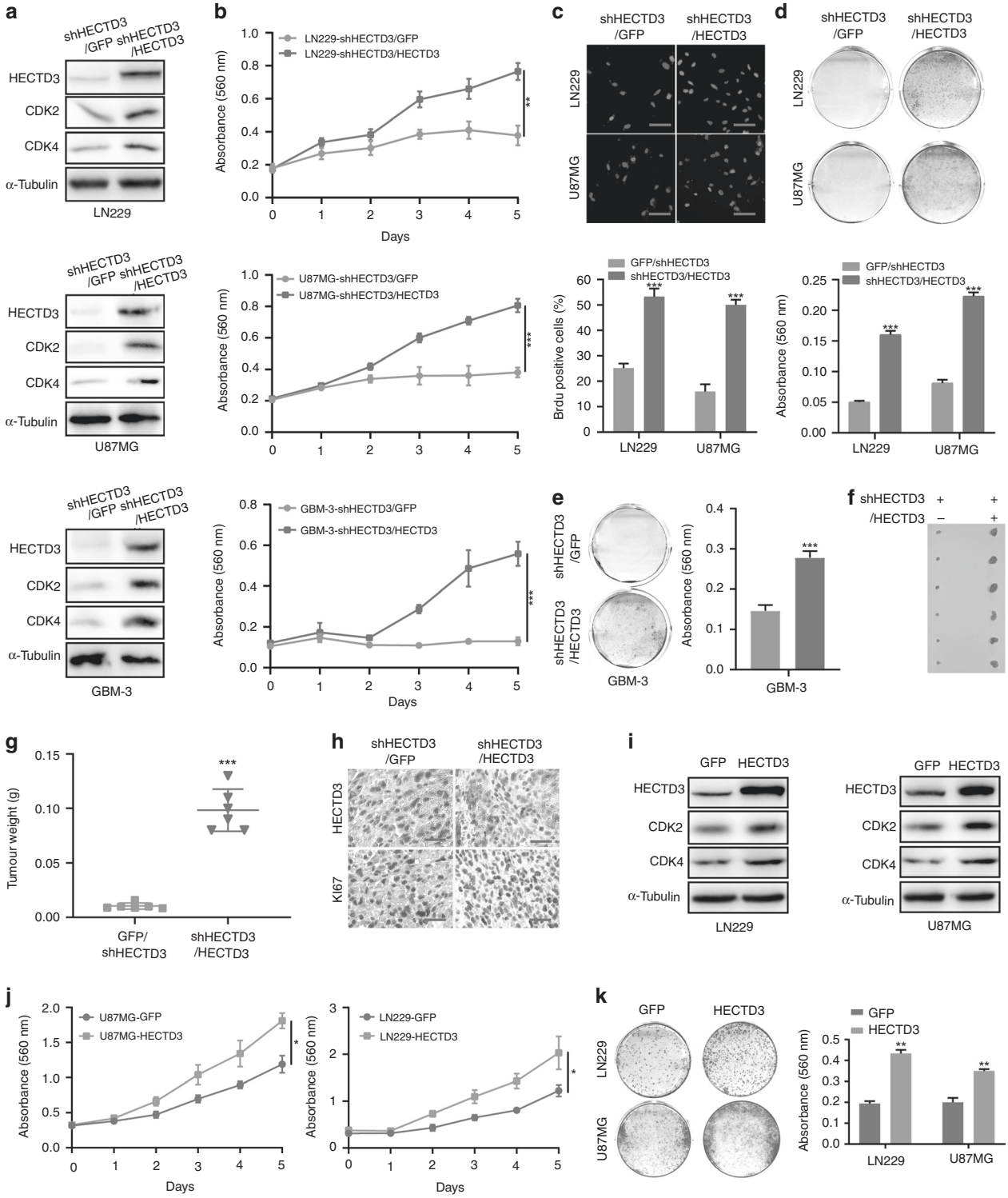

Fig. 3 HECTD3 is required for GBM cell proliferation. a Western blot assay was performed to detect the expression of cell cycle-related proteins CDK2 and CDK4 after restoring the expression of HECTD3 in HECTD3-knocked-down LN229 and U87MG cells. **b**–**e** MTT assay, BrdU incorporation experiments, and plate colony formation assays were successively performed to detect the effect of rescued HECTD3 expression in HECTD3-knocked-down and GBM cell proliferation. **f**, **g** Mice subcutaneous tumourigenesis experiment was used to detect the effect of rescued HECTD3 expression after the knockdown of HECTD3 on mice subcutaneous tumourigenesis ability of U87MG cells. **h** Immunohistochemistry was used to detect the effect of restored HECTD3 after knocking down HECTD3 on HECTD3 and Ki67. **i** Western blot assay was used to detect the effects of HECTD3 overexpression in cell cycle-associated proteins CDK2 and CDK4. **j**, **k** MTT and plate cloning assays were used to detect the effect of overexpressed HECTD3 on LN229 and U87MG cells proliferation. All data were expressed as mean ± SD. The Student's *t* test was performed to analyse the significance. $*p < 0.05$, $**p < 0.01$, $***p < 0.001$.

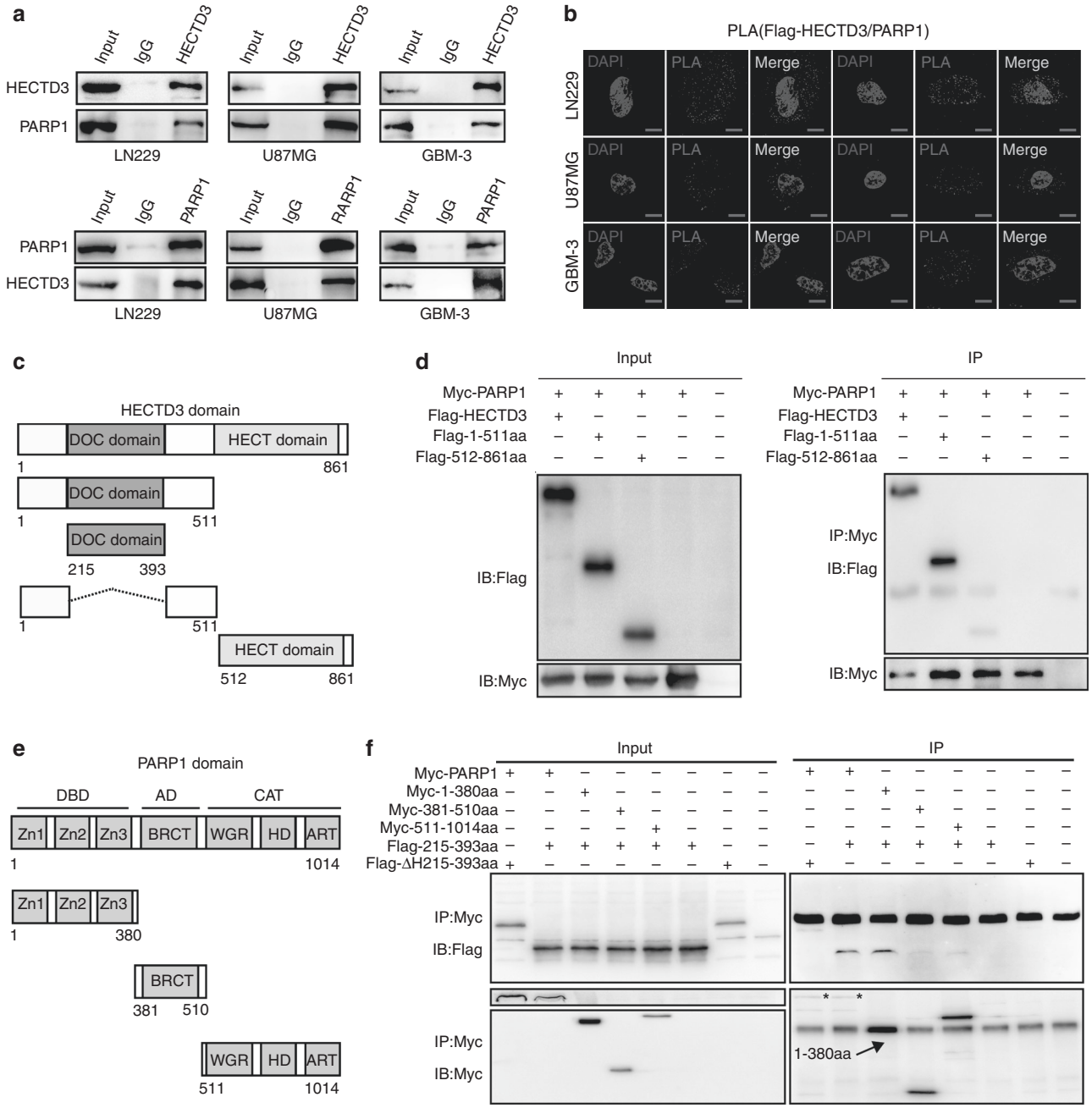

Fig. 4 The HECTD3 DOC domain interacts with the PARP1 DNA-binding domain. a Interaction between HECTD3 and PARP1 in LN229 and U87MG cells**. b** A PLA experiment was used to detect the interaction between HECTD3 and PARP1. **c** Graphs portraying HECTD3 DOC and HECT domains. **d** Interaction between PARP1 and HECTD3 truncated domains in 293 cells. **e** Diagram of PARP1 domains. **f** Interaction of DOC (amino acids 215–393), DOC lost domain (amino acids ΔH215–393) and PARP1 domains in 293 cells.

control, protein stability, and metastatic processes [31]. Then, apoptosis-related proteins (caspase-3 and cleaved-caspase-3) were detected by western blot, and the results indicated that the protein expression of cleaved-caspase-3 was increased in HECTD3 knockdown LN229, U87MG, and GBM-3 cells (Figs. 5d and S4E). Furthermore, the western blot assay indicated an increase in PARP1 expression level in GBM cells overexpressing HECTD3 compared to control cells (Fig. 5e). We further applied flow cytometry to detect the HECTD3 effect on cell apoptosis. The assay showed that the apoptosis of GBM cells with HECTD3 knockdown was increased (Fig. 5f). Phosphorylated histone H2AX (γH2AX) is an indicator of DNA damage. Immunofluorescence (IF) assays were performed to examine the γH2AX level and found that the number of cells with positive staining of γ-H2AX was significantly increased in HECTD3 knocked-down LN229 and U87MG cells versus control cells (Fig. 5g). We previously demonstrated that the HECTD3 interacted with the PARP1. Previous studies have shown that Cys823 of HECTD3 plays an ubiquitinase active site role [16, 32]. Therefore, to detect which domain of HECTD3 regulates the expression of PARP1, the DOC domain, HECT ubiquitin domain, the ubiquitin active site mutant (C823A) of HECTD3 and Flag-HECTD3 were transferred into GBM cells. The results showed that the DOC and HECT domains, as well as the ubiquitin active site mutant (C823A) of HECTD3, increased the expression of

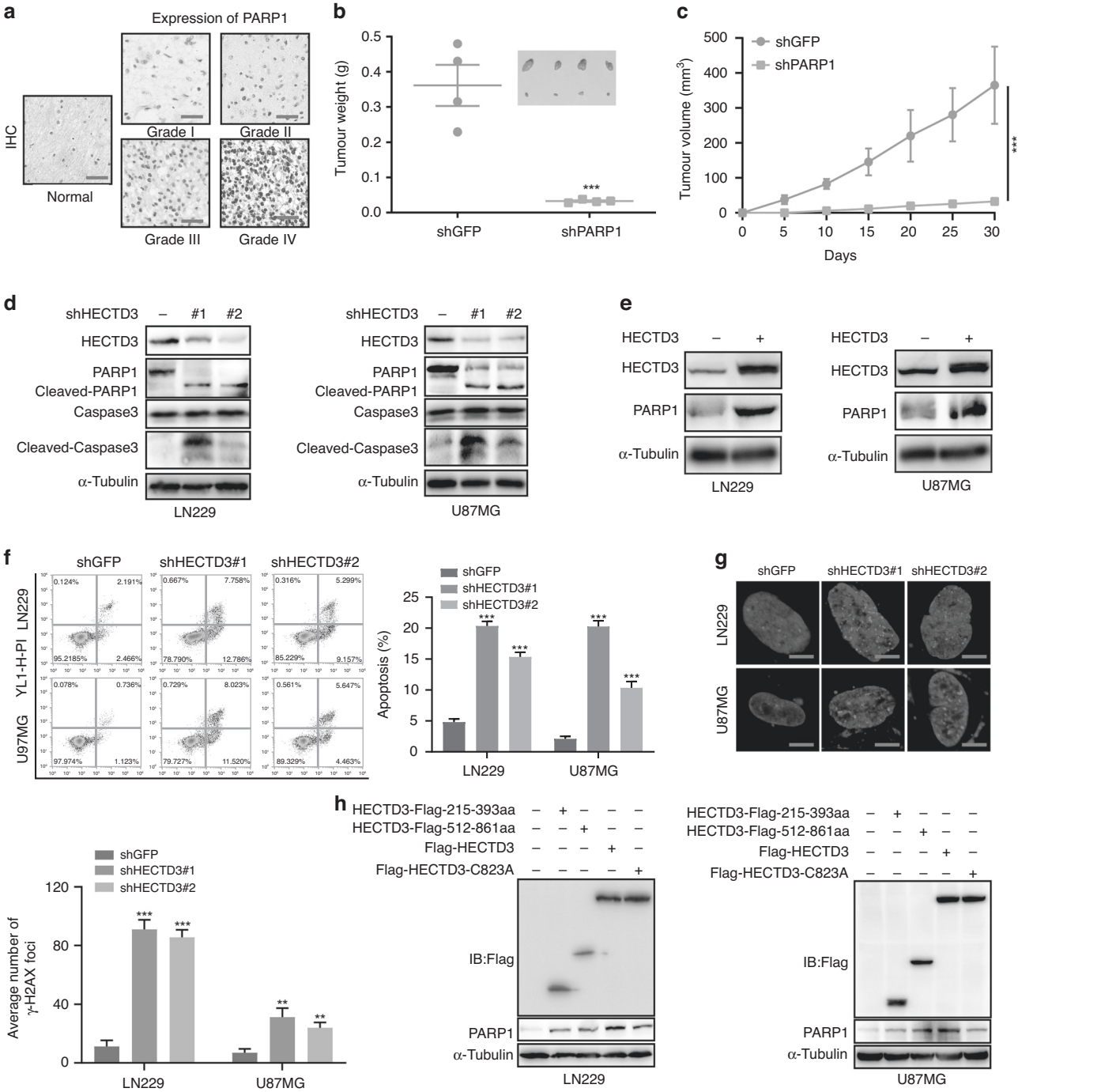

Fig. 5 Depletion of HECTD3 reduces the expression of PARP1 and induces apoptosis and DNA damage in GBM cells. **a** Immunohistochemical staining analysis detected PARP1 expression in 5 normal brain tissue samples and 35 glioma tissue samples. **b** The size and weight of xenograft tumours derived from PARP1-knocked-down U87MG cells were analysed. **c** The growth curves of tumours derived from PARP1-knocked-down U87MG cells were examined. **d** A western blot assay was performed to detect HECTD3, PARP1, cleaved PARP1, caspase-3, cleaved caspase-3, and α-Tubulin protein expressions in HECTD3-knocked-down LN229 and U87MG cells. **e** HECTD3 and PARP1 protein expression levels in HECTD3-overexpressing LN229 and U87MG cells were detected by western blot. **f** Flow cytometry analysis of apoptotic HECTD3-knocked-down LN229 and U87MG cells. **g** Immunofluorescence (IF) staining of γ-H2AX in HECTD3-knocked-down LN229 and U87MG cells. **h** The DOC-binding domain, HECT ubiquitin domain of HECTD3, HECTD3 C823A mutant (with a mutated ubiquitin active site), and Flag-HECTD3 were transferred into LN229 and U87MG cells to detect the protein expression of PARP1. All data were expressed as mean ± SD. The Student's *t* test was performed to analyse the significance. $^{**}p < 0.01$, $^{***}p < 0.001$.

PARP1. However, The simultaneous presence of HECT and DOC domains of HECTD3 enhanced PARP1 protein expression level (Fig. 5h). These data suggest that HECTD3 plays an important role in PARP1 regulation and is involved in GBM cell apoptosis and DNA damage.

HECTD3 mediates the K63-linked polyubiquitination of PARP1

PARP1 mRNA expression level was not significantly changed in HECTD3 knocked-down GBM cells (Fig. S4D). To further detect whether HECTD3 regulates PARP1 ubiquitination, knocked-down LN229, and U87MG cells were treated with MG132, and the

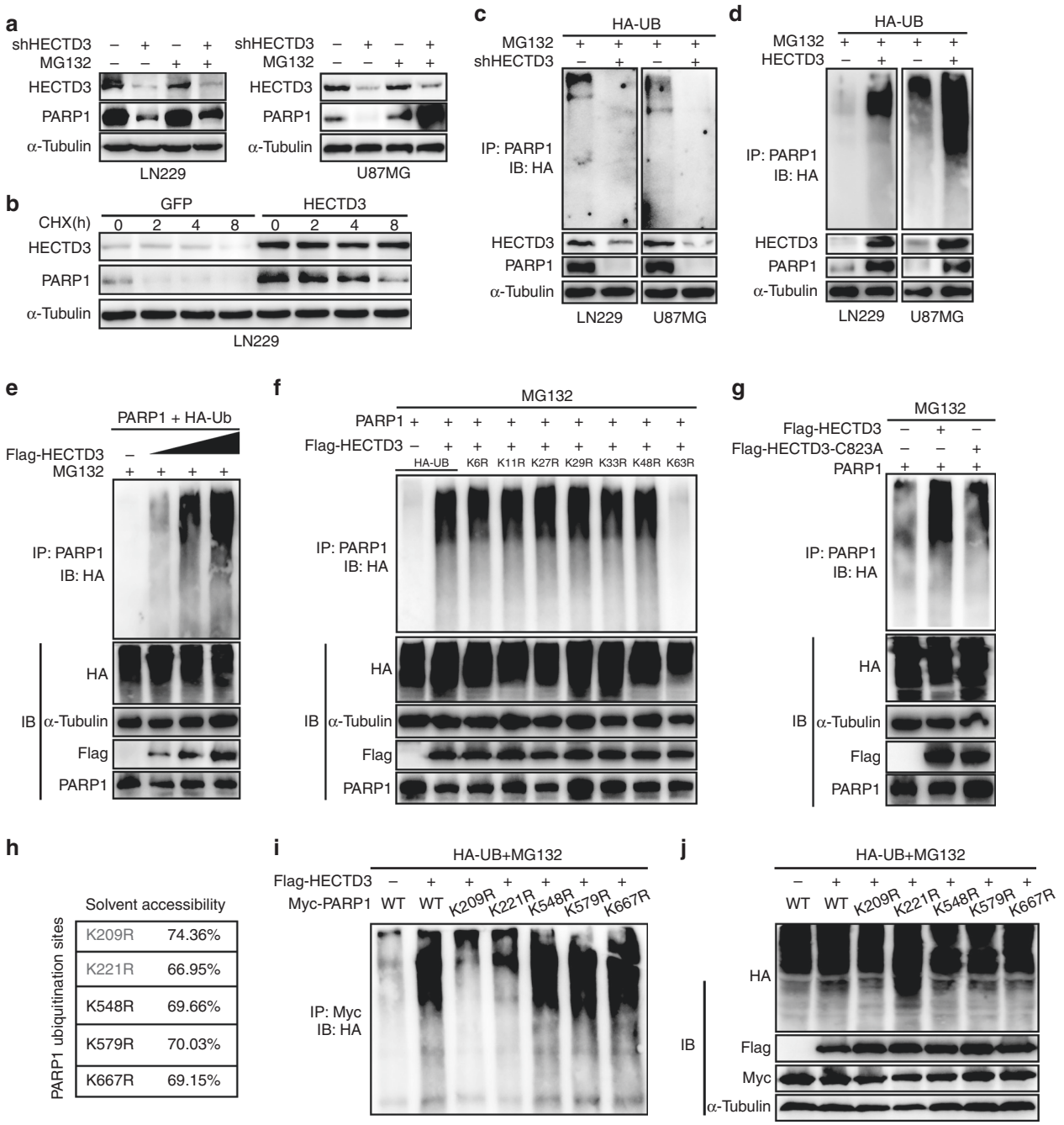

Fig. 6 HECTD3 mediates the K63-linked polyubiquitination of PARP1. a Cell lysates were prepared from knocked down HECTD3 cells that had been previously treated with or without MG132 for 7 h. **b** The PARP1 turnover rate of LN229 cells overexpressing HECTD3. **c**, **d** Ubiquitination assay of PARP1 in both HECTD3-knocked-down LN229 and U87MG cells and LN229 and U87MG cells overexpressing HECTD3. Equal amounts of cell lysates were immunoblotted with the indicated antibodies. **e** Lysates of 293 cells co-transfected with plasmids expressing MYC-PARP1 and HA-Ub and increasing amounts of Flag-HECTD3 were treated with MG132 immunoprecipitated with PARP1 beads and immunoblotted with an anti-HA antibody. **f** Constructed Flag-HECTD3, MYC-PARP1, HA-Ub, and ubiquitin mutant plasmids (K6R, K11R, K27R, K29R, K33R, K48R, K63R) were co-transferred in 293 cells for ubiquitination level assessments. **g** Lysates of 293 cells co-transfected with plasmids expressing MYC-PARP1, HA-Ub, Flag-HECTD3, and Flag-HECTD3-C823A for ubiquitination assay. **h**–**j** The Lys-based PARP1 mutants (K209R, K221R, K548R, K579R, and K667R) were co-transfected for ubiquitination assay. Predicted ubiquitin sites of PARP1 (http://140.138.144.145/~ubinet/index.php).

findings obtained showed a rescue of PARP1 protein expression level (Fig. 6a). Then, a ubiquitination assay was applied on LN229, U87MG and GBM-3 cells led to the observation that HECTD3 knockdown and HECTD3 overexpression in GBM cells reduced and increased the PARP1 ubiquitination level (Figs. 6c, d and S5A, B). Moreover, the use of de novo protein synthesis inhibitor cycloheximide (CHX) to detect the PARP1 turnover rate showed that the PARP1 degradation rate was slowed down in LN229 cells overexpressing HECTD3 (Fig. 6b). Interestingly, the same observation was obtained in a dose-dependent manner when assayed in vitro (Fig. 6e). Recent studies have shown that HECTD3 mediates the non-K48-linked polyubiquitin chain of STAT3, caspase-8, caspase-9, MALT1 and TRAF3 [9, 12–16]. We speculated that HECTD3 might affect PARP1 polyubiquitination. Then, the

constructed plasmids (HA-Ub-WT, K6R, K11R, K27R, K29R, K33R, K48R, K63R), Flag-HECTD3, and MYC-PARP1 were co-transfected into 293 cells for ubiquitination assessment. As shown in Fig. 6f, HECTD3 mediated the K63-linked polyubiquitination of PARP1. Since previous studies have shown that Cys823 of HECTD3 plays an important role in polyubiquitination [16, 32], we engineered a HECTD3 mutant plasmid (C823A) and co-transfected it with Flag-HECTD3, MYC-PARP1 and HA-Ub into 293 cells for relative ubiquitination levels assessment. The results suggested that polyubiquitination of PARP1 was significantly reduced after the Cys823 point mutation in HECTD3 (Fig. 6g). To further determine which Lys of PARP1 is specifically targeted by ubiquitin-related molecules, we further constructed five PARP1 mutants at different Lys's sites (sites K209R, K221R, K548R, K579R, and K667R) by predicting the substrate sites of PARP1 (Fig. 6h). The results showed that the polyubiquitination of PARP1 decreased after Lys mutations at positions 209 and 221, respectively (Fig. 6i, j). Collectively, these data suggest that HECTD3 mediates the K63-linked polyubiquitination of PARP1 and stabilises PARP1 expression by recruiting ubiquitin-related molecules to Lys209 and Lys221, in the PARP1 ubiquitin-binding site, respectively.

HECTD3 activates the EGFR-mediated signalling pathway through PARP1

Studies have shown that EGFR amplification prevails in GBM cells [20, 33–36] with mutations and rearrangements [37]. It is particularly urgent to detect the target of EGFR. GEPIA and TCGA database explorations showed that EGFR was highly expressed in GBM patients and associated with a poor prognosis (Fig. 7a). Similar observations in the brain and central nervous system (CNS) cancers were obtained when investigating the Oncomine database (Fig. S6A). Previous studies have shown that PARP1 inactivation inhibited the activation of the EGFR signalling pathway [26]. Therefore, we assumed that HECTD3 might activate the EGFR-mediated signalling pathway by regulating PARP1 polyubiquitination. To test this hypothesis, we detected EGFR, P-EGFR, and P-AKT expression levels in HECTD3-knocked-down LN229 and U87MG cells via western blot assay and found reduced expression levels of EGFR, P-EGFR, and P-AKT in HECTD3 knocked-down LN229 and U87MG cells (Fig. 7b). To further prove that HECTD3 might activate EGFR signalling pathway through PARP1 polyubiquitination, we determined the expression levels of EGFR signalling pathway-related proteins after overexpressing PARP1 in HECTD3-knocked-down GBM cells. The results showed that the expression level of EGFR, P-EGFR, and P-AKT significantly increased compared to the knocked-down HECTD3 LN229 and U87MG cells groups (Fig. 7c). By applying MTT and plate colony formation assays, we revealed a rescue of GBM cell proliferative ability when compared to that of the HECTD3-knocked-down GBM cell groups (Fig. 7d, e). Moreover, we performed in situ injections of U87MG cells in mice, and we found that depletion of HECTD3 inhibited tumour size and prolonged the survival of mice. Furthermore, overexpression of PARP1 in mice model after HECTD3 knockdown caused a significant increase in tumour size, associated with a considerable decrease in mice survival rate (Fig. 7f, g). Detection of HECTD3, PARP1, and EGFR expression levels were confirmed in HECTD3-knocked-down tumour cells compared to controls by using IHC. These PARP1 and EGFR expression levels significantly increased in mice tumours overexpressing PARP1 after HECTD3 knockdown (Fig. 7h). In addition, we mapped the molecular mechanism of HECTD3 mediated K63-linked polyubiquitination of PARP1 and in activated EGFR pathway (Fig. 7i). These data show that HECTD3 promotes the proliferation of GBM cells by polyubiquitinating PARP1 and activating the EGFR signalling pathway, and suggest that HECTD3 might be a potential target for the treatment of GBM patients.

DISCUSSION

GBM is a highly invasive and malignant primary solid tumour and is the deadliest and most difficult to treat glioma in adults [38–40]. In recent years, although research on GBM has been more in depth, its pathogenesis and molecular mechanism remain unclear. Therefore, it is particularly urgent to explore the pathogenesis and mechanism of action of GBM. Recent reports have shown that the E3 ubiquitin ligase HECTD3 is abnormally expressed in a variety of solid tumours and associated with development and progression. In view of that, we explored the possible role(s) of HECTD3 in GBM. In this study, we first demonstrated that HECTD3 is highly expressed in GBM tissue samples and that the prognosis of patients with high HECTD3 expression is poor (Fig. 1a). Furthermore, we showed that HECTD3 participated in the proliferation, apoptosis, DNA damage, and migration of GBM cells, which led us to assumed that HECTD3 might be a potential target for the treatment of GBM patients.

PARP1 is a founding member of the PARP family, and PARP1 plays an important role in chromatin remodelling, replication, transcription, energy metabolism, inflammatory response, and cell death. Studies have shown that PARP1 expression is regulated by a variety of cellular processes, such as phosphorylation, acetylation, and ubiquitination. By applying the IHC assay, we reported that PARP1 was highly expressed in GBM (Fig. 5a), and interacted directly with HECTD3 through their respective DNA binding (PARP1) and DOC (HECTD3) domains, respectively. We further revealed that HECTD3 mediated the K63-linked polyubiquitination of PARP1 and stabilised PARP1 and reported that the polyubiquitination of PARP1 was significantly reduced after mutating the Cys823 in the ubiquitin active site of HECTD3. Inversely, HECTD3 mediated K63-linked polyubiquitination of PARP1 and stabilised PARP1 expression by recruiting ubiquitin-related molecules to Lys209 and Lys221 in the ubiquitin-binding site of PARP1.

EGFR is highly expressed in more than half of the GBM gene analyses, and alterations include gene amplification and mutation [37]. It is of great clinical significance to identify the target(s) of EGFR. Previous studies have shown that the inactivation of PARP1 inhibited the activation of the EGFR signalling pathway [26]. In this study, we reported that HECTD3 activates the EGFR-mediated signalling pathway through the polyubiquitination of PARP1. These data indicate that the HECTD3-PARP1-EGFR axis might be a powerful target for the treatment of GBM patients.

It is of great significance to identify drugs targeting HECTD3 for the treatment of GBM. Studies have shown that HECTD3 promotes the occurrence and development of cancer and has anti-apoptotic characteristics [9]. The high expression of HECTD3 could enhance the tolerance of anti-tumour clinical drugs. Therefore, the research and development of HECTD3 inhibitors are urgent. Its combination with clinical drugs could improve the survival rate of cancer patients. Here, we found that PARP1 serves as a direct ubiquitin target of HECTD3 in GBM, and we found that the interaction between HECTD3 and PARP1 could promote PARP1-mediated tolerance to radiotherapy and chemotherapeutic drugs of tumours. Therefore, the combination of targeted drugs for HECTD3 and PARP1 could effectively improve the survival of tumour-suffering patients compared to the use of a one-targeting drug. We further reported that DOC and HECT domains increased PARP1 expressions. However, the simultaneous presence of these two domains enhanced PARP1 expression (Fig. 5h). Therefore, we speculated that these HECTD3 domains could counteract the degradation of PARP1 by other ubiquitin-related ligases or regulators and stabilise PARP1 expression.

Globally, this study demonstrated that HECTD3 mediates the K63-linked polyubiquitination of PARP1 and stabilises the latter expression by recruiting ubiquitin-related molecules to Lys209 and Lys221 in the ubiquitin-binding site of PARP1, and activates the EGFR-mediated signalling pathway, which promotes GBM tumourigenesis. Based on our research results, HECTD3 might be a

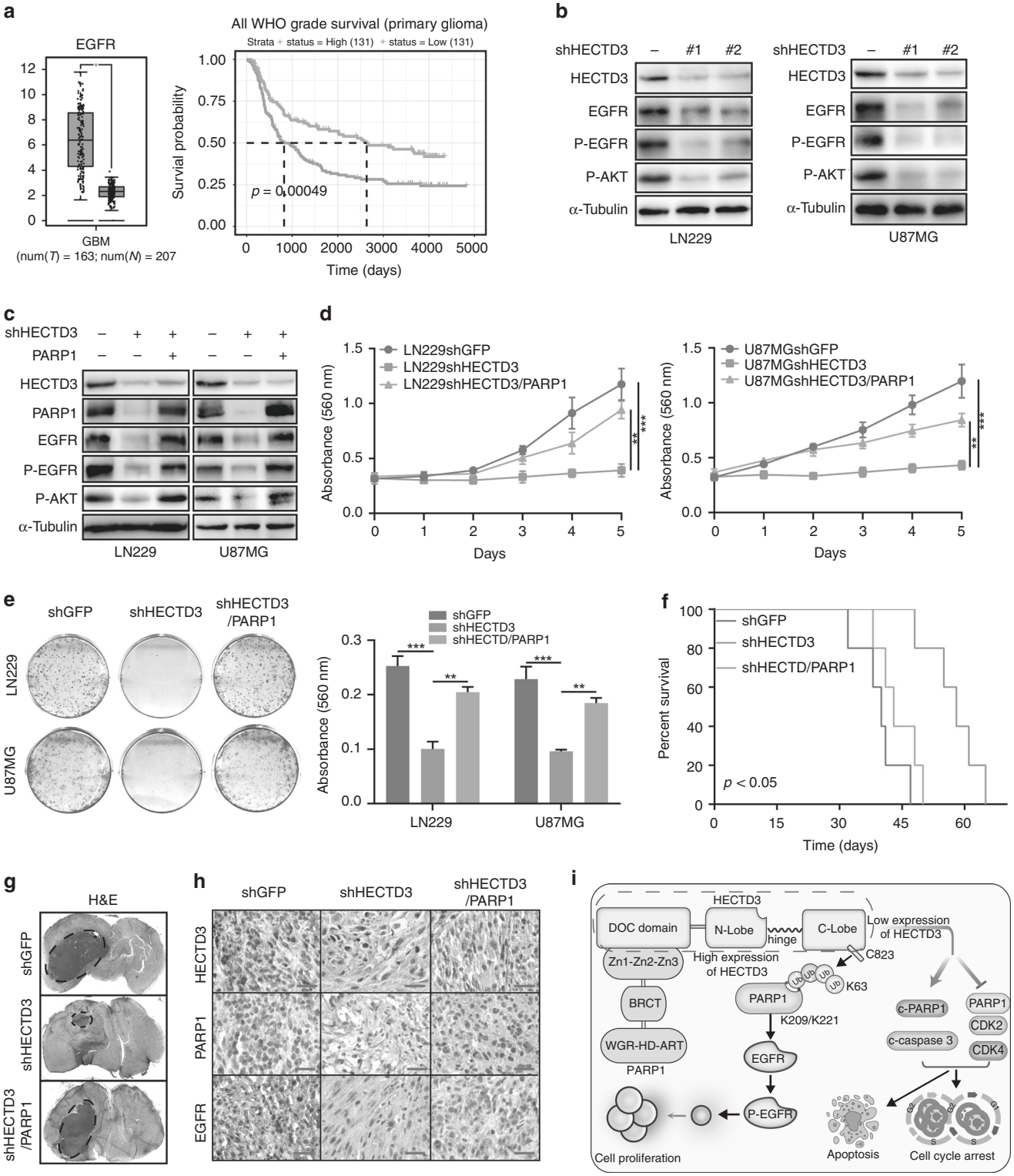

Fig. 7 HECTD3 activates the EGFR-mediated signalling pathway through PARP1. a GEPIA (http://gepia.cancer-pku.cn/index.html) and CGGA (http://www.cgga.org.cn/) databases were used to analyse the expression of EGFR expression in GBM and glioma-related patient prognosis. **b** HECTD3, EGFR, P-EGFR, P-AKT, and α-Tubulin protein expressions were detected by western blot in HECTD3-knocked-down LN229 and U87MG cells. **c** HECTD3, PARP1, EGFR, P-EGFR, P-AKT, and α-Tubulin expression levels were detected after overexpressing PARP1 in HECTD3-knocked-down LN229 and U87MG cells. **d** Resultant growth curves after overexpressing PARP1 in HECTD3-knocked-down LN229 and U87MG cells. cells. **e** The plate colony formation ability after overexpression of PARP1 in HECTD3-knocked-down LN229 and U87MG cells. **f**, **g** Mice survival curve and orthotopic tumourigenesis abilities after overexpression of PARP1 in HECTD3-knocked-down U87MG cells. **h** Expression levels of HECTD3, PARP1 and EGFR were detected by immunohistochemistry. **i** HECTD3 mediated K63-linked polyubiquitination of PARP1 and activated the EGFR pathway. All data were expressed as mean ± SD. The Student's *t* test was performed to analyse the significance. $^{*}p < 0.05$, $^{**}p < 0.01$, $^{***}p < 0.001$.

potential therapeutic target for the treatment of GBM-suffering patients, and the HECTD3–PARP1–EGFR axis represents a promising theoretical basis for clinical cancer research.

DATA AVAILABILITY

All data analysed or generated in this study are included in this article as well as in the Supplementary Information file.

REFERENCES

1. Budke M, Isla-Guerrero A, Perez-Lopez C, Perez-Alvarez M, Garcia-Grande A, Bello MJ, et al. A comparative study of the treatment of high grade gliomas. Rev Neurol. 2003;37:912–6.
2. Riddick G, Fine HA. Integration and analysis of genome-scale data from gliomas. Nat Rev Neurol. 2011;7:439–50.
3. Zhao Y, He J, Li Y, Lv S, Cui H. NUSAP1 potentiates chemoresistance in glioblastoma through its SAP domain to stabilize ATR. Signal Transduct Target Ther. 2020;5:44.
4. Jiang Q, Li F, Cheng Z, Kong Y, Chen C. The role of E3 ubiquitin ligase HECTD3 in cancer and beyond. Cell Mol life Sci. 2020;77:1483–95.
5. Pickart CM. Mechanisms underlying ubiquitination. Annu Rev Biochem. 2001;70:503–33.
6. Komander D, Rape M. The ubiquitin code. Annu Rev Biochem. 2012;81:203–29.
7. Tokunaga F, Sakata S, Saeki Y, Satomi Y, Kirisako T, Kamei K, et al. Involvement of linear polyubiquitylation of NEMO in NF-kappaB activation. Nat Cell Biol. 2009;11:123–32.
8. Trempe JF. Reading the ubiquitin postal code. Curr Opin Struct Biol. 2011;21:792–801.
9. Li Y, Chen X, Wang Z, Zhao D, Chen H, Chen W, et al. The HECTD3 E3 ubiquitin ligase suppresses cisplatin-induced apoptosis via stabilizing MALT1. Neoplasia. 2013;15:39–48.
10. Zhang L, Kang L, Bond W, Zhang N. Interaction between syntaxin 8 and HECTd3, a HECT domain ligase. Cell Mol Neurobiol. 2009;29:115–21.
11. Yu J, Lan J, Zhu Y, Li X, Lai X, Xue Y, et al. The E3 ubiquitin ligase HECTD3 regulates ubiquitination and degradation of Tara. Biochem Biophys Res Commun. 2008;367:805–12.
12. Shu T, Li Y, Wu X, Li B, Liu Z. Down-regulation of HECTD3 by HER2 inhibition makes serous ovarian cancer cells sensitive to platinum treatment. Cancer Lett. 2017;411:65–73.
13. Li Y, Wu X, Li L, Liu Y, Xu C, Su D, et al. The E3 ligase HECTD3 promotes esophageal squamous cell carcinoma (ESCC) growth and cell survival through targeting and inhibiting caspase-9 activation. Cancer Lett. 2017;404:44–52.
14. Li Z, Zhou L, Prodromou C, Savic V, Pearl LH. HECTD3 mediates an HSP90-dependent degradation pathway for protein kinase clients. Cell Rep. 2017;19:2515–28.
15. Li F, Li Y, Liang H, Xu T, Kong Y, Huang M, et al. HECTD3 mediates TRAF3 polyubiquitination and type I interferon induction during bacterial infection. J Clin Investig. 2018;128:4148–62.
16. Li Y, Kong Y, Zhou Z, Chen H, Wang Z, Hsieh YC, et al. The HECTD3 E3 ubiquitin ligase facilitates cancer cell survival by promoting K63-linked polyubiquitination of caspase-8. Cell Death Dis. 2013;4:e935.
17. Wu X, Li L, Li Y, Liu Z. MiR-153 promotes breast cancer cell apoptosis by targeting HECTD3. Am J Cancer Res. 2016;6:1563–71.
18. Engbrecht M, Mangerich A. The nucleolus and PARP1 in cancer biology. Cancers. 2020;12:1813.
19. Ghorai A, Mahaddalkar T, Thorat R, Dutt S. Sustained inhibition of PARP-1 activity delays glioblastoma recurrence by enhancing radiation-induced senescence. Cancer Lett. 2020;490:44–53.
20. Libermann TA, Nusbaum HR, Razon N, Kris R, Lax I, Soreq H, et al. Amplification, enhanced expression and possible rearrangement of EGF receptor gene in primary human brain tumours of glial origin. Nature. 1985;313:144–7.
21. Furnari FB, Fenton T, Bachoo RM, Mukasa A, Stommel JM, Stegh A, et al. Malignant astrocytic glioma: genetics, biology, and paths to treatment. Genes Dev. 2007;21:2683–710.
22. Cancer Genome Atlas Research Network. Comprehensive genomic characterization defines human glioblastoma genes and core pathways. Nature. 2008;455:1061–8.
23. Hou J, Deng Q, Zhou J, Zou J, Zhang Y, Tan P, et al. CSN6 controls the proliferation and metastasis of glioblastoma by CHIP-mediated degradation of EGFR. Oncogene. 2017;36:1134–44.
24. Hatanpaa KJ, Burma S, Zhao D, Habib AA. Epidermal growth factor receptor in glioma: signal transduction, neuropathology, imaging, and radioresistance. Neoplasia. 2010;12:675–84.
25. Felsberg J, Hentschel B, Kaulich K, Gramatzki D, Zacher A, Malzkorn B, et al. Epidermal growth factor receptor variant III (EGFRvIII) positivity in EGFR-amplified glioblastomas: prognostic role and comparison between primary and recurrent tumors. Clin Cancer Res. 2017;23:6846–55.
26. Lai Y, Kong Z, Zeng T, Xu S, Duan X, Li S, et al. PARP1-siRNA suppresses human prostate cancer cell growth and progression. Oncol Rep. 2018;39:1901–9.
27. Peng W, Shi S, Zhong J, Liang H, Hou J, Hu X, et al. CBX3 accelerates the malignant progression of glioblastoma multiforme by stabilizing EGFR expression. Oncogene. 2022;41:3051–63.
28. Hou J, Xu M, Gu H, Pei D, Liu Y, Huang P, et al. ZC3H15 promotes glioblastoma progression through regulating EGFR stability. Cell Death Dis. 2022;13:55.
29. Dong Z, Lei Q, Yang R, Zhu S, Ke XX, Yang L, et al. Inhibition of neurotensin receptor 1 induces intrinsic apoptosis via let-7a-3p/Bcl-w axis in glioblastoma. Br J Cancer. 2017;116:1572–84.
30. Xuan F, Huang M, Liu W, Ding H, Yang L, Cui H. Homeobox C9 suppresses Beclin1-mediated autophagy in glioblastoma by directly inhibiting the transcription of death-associated protein kinase 1. Neuro Oncol. 2016;18:819–29.
31. McPhee TR, McDonald PC, Oloumi A, Dedhar S. Integrin-linked kinase regulates E-cadherin expression through PARP-1. Dev Dyn. 2008;237:2737–47.
32. Li F, Liang H, You H, Xiao J, Xia H, Chen X, et al. Targeting HECTD3-IKKalpha axis inhibits inflammation-related metastasis. Signal Transduct Target Ther. 2022;7:264.
33. Brennan CW, Verhaak RG, McKenna A, Campos B, Noushmehr H, Salama SR, et al. The somatic genomic landscape of glioblastoma. Cell. 2013;155:462–77.
34. Furnari FB, Cloughesy TF, Cavenee WK, Mischel PS. Heterogeneity of epidermal growth factor receptor signalling networks in glioblastoma. Nat Rev Cancer. 2015;15:302–10.
35. Chaffanet M, Chauvin C, Laine M, Berger F, Chedin M, Rost N, et al. EGF receptor amplification and expression in human brain tumours. Eur J Cancer. 1992;28:11–7.
36. Libermann TA, Razon N, Bartal AD, Yarden Y, Schlessinger J, Soreq H. Expression of epidermal growth factor receptors in human brain tumors. Cancer Res. 1984;44:753–60.
37. Eskilsson E, Rosland GV, Solecki G, Wang Q, Harter PN, Graziani G, et al. EGFR heterogeneity and implications for therapeutic intervention in glioblastoma. Neuro Oncol. 2018;20:743–52.
38. Gilbert MR, Dignam JJ, Armstrong TS, Wefel JS, Blumenthal DT, Vogelbaum MA, et al. A randomized trial of bevacizumab for newly diagnosed glioblastoma. N. Engl J Med. 2014;370:699–708.
39. Preusser M, Lim M, Hafler DA, Reardon DA, Sampson JH. Prospects of immune checkpoint modulators in the treatment of glioblastoma. Nat Rev Neurol. 2015;11:504–14.
40. Alexander BM, Cloughesy TF. Adult glioblastoma. J Clin Oncol. 2017;35:2402–9.

ACKNOWLEDGEMENTS

We thank Daping Hospital (Chongqing, China) for providing primary glioblastoma cells (GBM-3). We thank Dr. Ulrich Aymard Ekomi Moure for correcting spelling and grammar errors. We also thank Jifu Li for providing technical support during the use of the Confocal Laser Scanning Microscope (Olympus Fv1000, Japan).

AUTHOR CONTRIBUTIONS

GZ and HC were responsible for the design of the study. GZ, PL, RT, SW, BL, and XH performed the experiments. HC, GZ, XD, RY, and EZ analysed the data and designed the figures. GZ, PL, and JZ wrote the manuscript.

FUNDING

This research was supported by the Natural Science Foundation of Chongqing (cstc2022ycjh-bgzxm0145) and (cstc2019jcyjzdxmX0033).

COMPETING INTERESTS

The authors declare no competing interests.

ETHICS APPROVAL AND CONSENT TO PARTICIPATE

Animal handling was approved by the Committee for Animal Protection and ethics of Southwest University. All experiments were conducted following the Guidelines for Animal Health and Use of the Ministry of Science and Technology of China (2006). Clinical glioma tissue samples were purchased from Chaoying Biotechnology Co., Ltd, and the study was approved by the Medical Ethics Committee of Tongxu County People's Hospital of Henan Province and all participants provided informed consent.

ADDITIONAL INFORMATION

Supplementary information The online version contains supplementary material available at https://doi.org/10.1038/s41416-022-01970-9.

Correspondence and requests for materials should be addressed to Ping Liang or Hongjuan Cui.

Reprints and permission information is available at http://www.nature.com/reprints

Publisher's note Springer Nature remains neutral with regard to jurisdictional claims in published maps and institutional affiliations.

Springer Nature or its licensor holds exclusive rights to this article under a publishing agreement with the author(s) or other rightsholder(s); author self-archiving of the accepted manuscript version of this article is solely governed by the terms of such publishing agreement and applicable law.